Published in final edited form as:
J Invest Dermatol. 2014 October ; 134(10): 2570–2578. doi:10.1038/jid.2014.164.

Epithelial inflammation resulting from an inherited loss-of-function mutation in *EGFR*

Patrick Campbell[1,10], **Penny Morton**[2,10], **Takuya Takeichi**[1,4], **Amr Salam**[1], **Nerys Roberts**[5], **Laura E. Proudfoot**[1], **Jemima E. Mellerio**[1,6], **Kingi Aminu**[5], **Cheryl Wellington**[5], **Sachin N. Patil**[5], **Masashi Akiyama**[4], **Lu Liu**[7], **James R. McMillan**[7], **Sophia Aristodemou**[7], **Akemi Ishida-Yamamoto**[8], **Alya Abdul-Wahab**[1], **Gabriela Petrof**[1], **Kenneth Fong**[1], **Sarawin Harnchoowong**[1], **Kristina Stone**[3], **John I. Harper**[6], **W. H. Irwin McLean**[9], **Michael A. Simpson**[3], **Maddy Parsons**[2,11], and **John A. McGrath**[1,9,11]

[1]St John's Institute of Dermatology, King's College London, London, UK

[2]Randall Division of Cell and Molecular Biophysics, King's College London, London, UK

[3]Department of Medical and Molecular Genetics, King's College London, London, UK

[4]Department of Dermatology, Nagoya University Graduate School of Medicine, Nagoya, Japan

[5]Department of Paediatrics, Chelsea and Westminster Hospital NHS Foundation Trust, London, UK

[6]Department of Paediatric Dermatology, Great Ormond Street Hospital for Children NHS Foundation Trust, London, UK

[7]GSTS Pathology, St Thomas' Hospital, London, UK

[8]Department of Dermatology, Asahikawa Medical University, Asahikawa, Japan

[9]Dermatology and Genetic Medicine, University of Dundee, Dundee, UK

Abstract

Epidermal growth factor receptor (EGFR) signaling is fundamentally important for tissue homeostasis through EGFR/ligand interactions that stimulate numerous signal transduction pathways. Aberrant EGFR signaling has been reported in inflammatory and malignant diseases but thus far no primary inherited defects in EGFR have been recorded. Using whole-exome sequencing, we identified a homozygous loss-of-function missense mutation in *EGFR* (c. 1283G>A; p.Gly428Asp) in a male infant with life-long inflammation affecting the skin, bowel and lungs. During the first year of life, his skin showed erosions, dry scale, and alopecia. Subsequently, there were numerous papules and pustules – similar to the rash seen in patients

Correspondence: John McGrath, Dermatology Research Labs, Floor 9 Tower Wing, Guy's Hospital, Great Maze Pond, London SE1 9RT, UK. Tel: 44-20-71886409; Fax: 44-20-71888050; john.mcgrath@kcl.ac.uk.
[10]Joint first authors
[11]Joint senior authors

CONFLICT OF INTEREST
The authors state no conflict of interest.

Europe PMC Funders Author Manuscripts

receiving EGFR inhibitor drugs. Skin biopsy demonstrated an altered cellular distribution of EGFR in the epidermis with reduced cell membrane labeling, and *in vitro* analysis of the mutant receptor revealed abrogated EGFR phosphorylation and EGF-stimulated downstream signaling. Microarray analysis on the patient's skin highlighted disturbed differentiation/premature terminal differentiation of keratinocytes and upregulation of several inflammatory/innate immune response networks. The boy died aged 2.5 years from extensive skin and chest infections as well as electrolyte imbalance. This case highlights the major mechanism of epithelial dysfunction following EGFR signaling ablation and illustrates the broader impact of EGFR inhibition on other tissues.

INTRODUCTION

EGFR signaling represents a key activity in several biologic processes underpinning tissue development and homeostasis (Jutten and Rouschop, 2014). Thus far, 7 EGFR ligands have been identified: EGF, transforming growth factor-α, amphiregulin, heparin-binding EGF-like growth factor, betacellulin, epiregulin, and epigen (Schneider and Wolf, 2009; Nanba *et al*., 2013). Interaction between EGFR and these ligands leads to stimulation of numerous transduction pathways that includes the RAS/RAF/MEK/ERK, PLC-gamma/PKC, PI3K/AKT, JAK/STAT, and NF-κB cascades (Jost *et al.*, 2000; Silbilia *et al.*, 2007). Acquired abnormalities of EGFR signaling have been observed in various inflammatory and malignant diseases (Jost *et al.*, 2000; Gschwind *et al.*, 2004; Dreux *et al.*, 2006; Zhang *et al*., 2014). Of note, aberrant EGFR activation is found in many tumor cells, and humanized neutralizing antibodies and synthetic small compounds against EGFR are in clinical use today. These drugs may cause skin and hair toxicities, indicating a key role for EGFR in cutaneous homeostasis (Lacouture, 2006; Liu *et al*., 2013). These side-effects have been recapitulated in a mouse model, with evident abnormalities in cutaneous chemokines associated with early infiltration of macrophages and mast cells and later infiltration of eosinophils, T cells and neutrophils (Mascia *et al*., 2013). *EGFR* mutations in tumors are typically gain-of-function and located within the tyrosine kinase domain of the protein, but thus far there are no reports of naturally occurring loss-of-function mutations in humans. Knockout and transgenic murine models and *in vitro* studies have demonstrated the essential role of EGFR in multiple organs (Miettinen *et al.*, 1995; Silbia and Wagner, 1995; Threadgill *et al.*, 1995; Jost *et al.*, 2000; Schneider *et al.*, 2008), but clinical correlates in patients are currently lacking. In this study, we used whole-exome sequencing to identify an inherited loss-of-function mutation in *EGFR* in an individual with inflammatory skin, lung and bowel disease.

RESULTS AND DISCUSSION

Clinical presentation with cutaneous erosions and inflammation

We investigated a male infant born to parents of Polish Roma origin who presented to us at 12 months of age with extensive skin inflammation. Initially, there were widespread erosions affecting his trunk and limbs that had been present since birth (Figure 1a), but subsequently we observed papules and pustules (Figure 1b). He also had life-long watery diarrhea and respiratory difficulties. He was born at 34 weeks' gestation, weighing 1560

grams; the pregnancy had been complicated by polyhydramnios and maternal hypertension. Clinically, at 12 months his weight was only 5.52kg with evident failure to thrive. His inflamed skin was frequently infected with *Staphylococcus aureus*. He had loss of scalp hair but long eyelashes (trichomegaly). No nail abnormalities were observed. He had previously undergone surgery for probable coarctation of the aorta and was noted to be hypertensive. Other abnormalities included recurrent bronchiolitis and pulmonary infection with *Pseudomonas aeruginosa* (requiring tracheostomy and oxygen). Renal ultrasound showed bilateral renal enlargement but no obstruction. The child had no specific food allergies but was unable to tolerate solids due to diarrhea and vomiting and severe dehydration. We observed low albumin, zinc, vitamin A, iron, magnesium, profound hypokalaemia (persistent), and hypernatraemia - though barium meal showed no evidence of malabsorption. He preferred to drink water rather than milk and subsequently required total parenteral nutrition. Blood eosinophil counts were slightly elevated during the first year (observed levels 0.4-1.0 × 10^9/l). Total IgE was found to be raised as a neonate (100 IU/l; range for <1 year 0-15 IU/l) and at 15 months (107 IU/l; range for this age 0-60 IU/l). IgM was borderline normal/low; IgG and IgA were normal. Venous access lines frequently became clotted and he developed deep vein thromboses. He died aged 2.5 years as a result of cutaneous and pulmonary infections and electrolyte imbalance. Further details of the clinical history can be found in the Supplementary Material.

Skin biopsy reveals acanthosis and intra-epidermal edema

We obtained written informed consent from the subject's legal guardian with approval from the St. Thomas' Hospital Ethics Committee. Elliptical skin biopsies were obtained under local anesthetic from a non-lesional area on the right thigh of the child (aged 12 months) as well as the abdomens of healthy control patients undergoing cosmetic ("tummy tuck") surgery. The initial clinical diagnosis was a subtype of inherited skin fragility, a heterogeneous group of disorders known collectively as epidermolysis bullosa (EB) (Fine *et al.*, 2008). Light microscopy of non-lesional skin revealed mild acanthosis compared to age- and site-matched control skin, as well as a slight widening between adjacent keratinocytes (Figure 2a). A few neutrophils were noted within the superficial dermis with some infiltration of follicular epithelium and folliculitis, although Gram stain for bacteria was negative. The changes within the epidermis resembled those of a primary inherited abnormality of desmosomes (Petrof *et al.*, 2012), although transmission electron microscopy showed intercellular edema from the basal layer to the mid-spinous layer and a slight decrease in the number of gap junctions but no structural or numerical abnormalities in hemidesmosome or desmosome cell junctions (Figure 2b). Skin immunolabeling using a panel of antibodies that target basement membrane and epidermal proteins implicated in inherited skin fragility disorders (see Supplementary Material for antibody details) demonstrated a marked reduction in staining intensity for the desmosomal proteins desmoglein 1 and plakophilin 1, as well as altered labeling patterns for profilaggrin, involucrin and keratin 10, markers of terminal differential in the epidermis (illustrated in Supplementary Material). Some of the clinicopathologic features also resembled Netherton syndrome, an autosomal recessive disorder associated with loss-of-function mutations in a serine protease inhibitor (*SPINK5*) that encodes lympho-epithelial Kazal-type related inhibitor (LEKT1) (Chavavas *et al.*, 2000; Stoll *et al.*, 2001). Immunostaining for LEKTI in

our patient's skin, however, revealed a slight increase compared to control (illustrated in Supplementary Material)– in contrast to findings of reduced LEKTI expression that usually accompany Netherton syndrome. Taken together, these findings were not in keeping with any known form of EB, Netherton syndrome or any other recognized inherited or acquired skin disease.

Whole-exome sequencing reveals a homozygous missense mutation in *EGFR*

Next, after obtaining approval from the ethics committee and informed consent, we extracted genomic DNA from peripheral blood samples from the child, other family members and controls in compliance with the Helsinki Guidelines. Using the patient's DNA, whole-exome sequencing was performed on the Illumina HiSeq 2000 (San Diego, CA, USA). After excluding pathogenic mutations in genes implicated in different forms of EB (Fine *et al.*, 2008), the exome variant profile was filtered to look for novel homozygous mutations (based on probable consanguinity). This disclosed 6 possible gene mutations (see Supplementary Material). Within these genes, *EGFR* was deemed to be of potential relevance given that some clinical features (e.g. papulo-pustular skin eruptions, alopecia and trichomegaly) resembled known side-effects of EGFR inhibitor drugs (Lacouture, 2006). Immunofluorescence microscopy to assess EGFR expression in the affected infant's skin showed a markedly altered staining pattern with loss of the cell peripheral membrane labeling and a more cytoplasmic or peri-nuclear region distribution, compared to strong cell membrane localization of EGFR throughout the epidermis, with minimal intracellular labeling, in control skin (Figure 2c). The non-synonymous substitution identified in exon 11 of *EGFR*, c.1283G>A, replaces a neutral glycine with a negatively charged aspartic acid molecule at a highly conserved residue, p.Gly428Asp. The pathogenicity of this missense mutation was supported by both the 'Sorts Intolerant From Tolerant' (SIFT; score 0, probably damaging) and Polymorphism Phenotyping v2 (polyphen-2; score 1, probably damaging) programs (Ng and Henikoff, 2003; Adzhubei *et al.*, 2010). The *EGFR* mutation was also validated by Sanger sequencing (Figure 2d; primers for *EGFR* amplification are given in Supplementary Material) and found to be homozygous in the affected patient, heterozygous in the mother, and homozygous wild-type sequence in the unaffected older sibling; DNA from the father was not available. The mutation is located in extracellular domain III of EGFR (Figure 2e), in contrast to the tyrosine kinase domain mutations commonly found in tumors (Kumar *et al.*, 2008). The region surrounding the mutation has been postulated to be involved in intra-molecular interactions that promote dimerization of EGFR and receptor activation (Ogiso *et al.*, 2002; Dawson *et al.*, 2005). We were unable to find the observed mutation in the dbSNP database, the 1000 Genomes database, the 13,005 exomes in the Exome Variant Server or in 900 unrelated European in-house control exomes.

Aberrant cutaneous expression of genes germane to keratinocyte differentiation, inflammatory response and innate immunity

Microarray data have been deposited in the Gene Expression Omnibus repository; accession number GSE54162. Comparison of the affected infant's skin with healthy control skin identified 2-fold or greater differential expression for 2,157 gene transcripts: 1004 up-regulated and 1153 down-regulated. These genes did not include *EGFR*, which was insignificantly up-regulated in the patient's skin (fold change=1.36; p=0.012). Evaluation of

the changes in gene expression by functional enrichment analysis identified a multitude of enriched gene ontology (GO) pathways, processes, networks and disease-associated transcripts germane to EGFR signaling (see Supplementary Materials for tabulated results). The top 3 up-regulated GO processes were linked to known EGFR functionality: keratinocyte differentiation, keratinization and epidermis development (involving genes such as transglutaminases, small proline rich genes, S100 genes, involucrin and late cornified envelope genes). Reports have also indicated a role for EGFR in regulating skin inflammation and cutaneous defence (Lichtenberger *et al.*, 2013; Mascia *et al.*, 2013). Thus, innate inflammatory response gene components (specifically PLA2, NF-κB, and JNK1) were among the most significantly up-regulated GO networks. Notably, *CCL2* expression was increased 2.2 fold, in keeping with reported findings in mouse models lacking epidermal *Egfr* expression (Lichtenberger *et al*., 2013). Additionally, regulation of epithelial-to-mesenchymal transition and angiogenesis, processes known to be controled by EGFR activation (Perrotte *et al.*, 1999; Avraham and Yarden, 2011), were identified as significantly down-regulated GO pathways and processes, respectively. Of note, there was also down-regulation of transcripts that are normally increased in tumors which show gain-of-function mutations in *EGFR* (e.g. non-small cell lung cancer, colorectal cancer, and glioblastoma).

Mutant EGFR at the plasma membrane is highly unstable and more susceptible to constitutive endocytosis

To determine whether the mutation p.Gly428Asp in *EGFR* was responsible for mislocalization of EGFR in the affected infant, we generated DNA constructs containing mutant or wild-type *EGFR* sequence linked to green fluorescent protein (GFP) and expressed these constructs in MCF7 cells that express low endogenous EGFR and analyzed EGF-dependent localization of EGFR using confocal microscopy. Under normal growth conditions, the mutant *EGFR* construct localized diffusely throughout the cytoplasm of the cell in contrast to the wild-type construct, which was present mostly on the plasma membrane (Figure 3a). EGF stimulation resulted in robust translocation of wild-type EGFR to the plasma membrane within 10 minutes of EGF treatment (Figure 3b). Conversely, the mutant EGFR remained in the cytoplasm following EGF stimulation with no clear recruitment to the plasma membrane (Figure 3b), suggesting this mutation prevents or diminishes EGFR membrane localization, supporting the immunostaining findings in patient skin (Figure 2c).

EGFR membrane localization is regulated through a balance of endocytosis under the control of a number of intracellular signaling pathways that converge on the large GTPase dynamin (Lee *et al.*, 2006). To examine whether the lack of mutant EGFR localization to the cell membrane was due to defective endocytic traffic, MCF-7 cells expressing either wild-type or mutant EGFR were treated with an inhibitor of dynamin-mediated endocytosis, Dynasore (Macia *et al.*, 2006). Receptor localization was then examined by confocal microscopy. In the absence of ligand, membrane localization of both wild-type and mutant EGFR increased after treatment with Dynasore (Figure 3c). Similar results were observed in a normal human keratinocyte cell line expressing wild-type or mutant EGFR (see Supplementary Material). Immunostaining of MCF-7 cells expressing wild-type or mutant

EGFR was performed using an antibody against the extracellular domain of EGFR to quantify membrane localization. Pearson's correlation coefficient analysis to quantify the co-localization between wild-type or mutant EGFR with the antibody staining demonstrated that for both constructs the EGFR membrane localization increased significantly following Dynasore treatment (Figure 3c) but not following treatment with the chemical chaperone 4-PBA (data not shown). These data demonstrate that the mutant EGFR is able to undergo recycling to the plasma membrane but that it can only be retained at the membrane upon blockade of endocytic signaling. This suggests that the mutation p.Gly428Asp renders EGFR at the plasma membrane highly unstable and thus more susceptible to constitutive endocytosis.

Loss of downstream Akt and ERK signaling associated with mutant EGFR

Following EGF binding, EGFR undergoes rapid autophosphorylation and activation at a number of residues within the cytoplasmic domain of the receptor. These changes result in recruitment of a host of initiators and scaffolds of signaling leading to activation of MAP kinase family members including ERK (p44/42) and Akt (Avraham and Yarden, 2011). We therefore assessed the effect of the mutation p.Gly428Asp on EGF dependent phosphorylation of EGFR and downstream signaling. EGF-dependent ERK and Akt activation were assessed in untransfected MCF-7 cells or those expressing wild-type or mutant EGFR. EGF-stimulated activation of EGFR (monitored by a phospho-specific antibody) was robust in the cells expressing wild-type EGFR, but was undetectable in the mutant EGFR-expressing cells above levels seen in untransfected controls (Figure 4a). Similarly, neither Akt nor ERK activation was detected following ligand binding in mutant EGFR-expressing cells, in contrast to cells expressing wild-type EGFR which showed robust EGF-stimulated EGFR, ERK and Akt phosphorylation (Figure 4a). We observed similar results in parallel experiments in another cell line (CHO-K1 cells) (see Supplementary Material for data).

The suppression of EGFR-dependent activation and downstream signaling observed suggests that the EGFR mutation p.Gly428Asp results in loss-of-function as well as loss of plasma membrane localization. One of the primary functions of EGFR signaling following EGF binding is to promote cell proliferation (Jost *et al.*, 2000). To determine whether the loss of EGF-dependent signaling in p.Gly428Asp mutant EGFR-expressing cells results in functional defects, proliferation was analyzed in CHO-K1 cells expressing the wild-type or mutant EGFR constructs. EGF and serum-stimulated proliferation was induced in CHO-K1 cells expressing wild-type EGFR, but no induction of cell growth was detected in cells expressing the mutant EGFR (Figure 4b). Indeed, there was a negative growth rate of the mutant EGFR-expressing cells, consistent with other work showing inhibition of EGFR signaling induces apoptosis in keratinocytes (Figure 4c) (Rodeck *et al.*, 1997).

Clinicopathologic overlap with patients harboring mutations in *ADAM17*

The exact mechanism by which the missense mutation p.Gly428Asp leads to loss of EGFR function is unclear. Mutagenesis of the adjacent amino acid (p.Arg429Glu) was previously found to prevent EGFR homo-dimerization through disruption of an interface between domains II and III of the protein (Dawson *et al.*, 2005). However, altered homo-dimerization

would not provide a sufficient explanation for the pathology as both monomeric EGFR and the p.Arg429Glu mutant were present at the plasma membrane (Ogiso *et al.*, 2002). In our experiments, we found that inhibition of endocytosis promoted levels of mutant EGFR at the cell surface. We hypothesize that the mutant receptor is unstable and rapidly undergoes internalization from the plasma membrane, perhaps implicating altered intracellular protein binding and subsequent aberrant tethering within membrane microdomains.

Functionally, failure of EGFR to correctly localize to cell membrane is expected to reduce ligand binding. In healthy people, several ligands require proteolytic cleavage to become capable of binding to EGFR – this ectodomain shedding is induced by at least 5 different metalloprotease enzymes, including ADAM17 (Blobel, 2005) – mutations in which may underlie an inflammatory skin and bowel disease that has overlap with the clinical features present in our patient (Blaydon *et al.*, 2011). We hypothesize that the lack of EGFR localization at the cell membrane in our patient has some similarity at a signaling level to that which occurs in the ADAM17-deficient patients, i.e. a common failure of EGFR-ligand interaction and altered downstream signal transduction.

Clinicopathologic similarities with mouse models of EGFR impairment

The clinical manifestations of the mutation p.Gly428Asp in terms of loss of EGFR function show some similarities with the phenotype of *Egfr* knockout or transgenic mice (Miettinen *et al.*, 1995; Silbia and Wagner, 1995; Threadgill *et al.*, 1995; Schneider *et al.*, 2008). Although the phenotype of *Egfr*-deficient mice depends on the strain of the mice (several are embryonic lethal), the abnormalities in the skin, lung and bowel in surviving mice are similar to many of the clinical manifestations in our patient. In the epidermis, some knockout mice show an initially thin skin that then becomes thicker but with defective barrier function (Miettinen *et al.*, 1995). Lack of *Egfr* in mice also affects hair growth, with wavy or reduced hair growth; EGFR is essential for normal hair follicle progression through the anagen, catagen, and telogen phases of the hair growth cycle (Hansen *et al.*, 1997; Schneider *et al.*, 2008). EGFR initiates hair growth and hair follicle organization, and EGFR inhibition leads to inflammation, follicular necrosis and alopecia, as well as slow hair growth with brittle hairs, as observed in our patient (Hansen et al., 1997; Schneider *et al.*, 2008). *Egfr*-deficient mouse lungs show condensed collapsed alveoli with a lack of surfactant leading to respiratory difficulty that has been likened to human neonatal respiratory distress syndrome (Miettinen *et al.*, 1995). In murine bowel lacking Egfr, there are fewer, shorter intestinal villi and reduced proliferation of jejunal enterocytes, leading to fluid loss (Miettinen *et al.*, 1995). Other abnormalities noted in the mice that show phenotypic similarities to our patient have included cystic dilatation of the collecting ducts in the kidneys (indicating that EGFR is vital for the differentiation of structures derived from the ureteric bud), aortic narrowing and a thrombotic tendency (Miettinen *et al.*, 1995). In addition, there are similarities in the phenotype of transgenic *Egfr*-and *Adam17* mice, thus supporting the clinical overlap in humans with germline autosomal recessive mutations in *EGFR* or *ADAM17* (Peschon *et al.*, 1998).

Clinical resemblance to the side-effects of EGFR inhibitor medications

The clinical manifestations in the child homozygous for p.Gly428Asp in *EGFR* also show some resemblance to the side-effect profile in individuals taking EGFR inhibitors. The side-effects of these drugs include a distinctive acne-like rash with pustules, dry skin, alopecia, trichomegaly, as well as mucositis, diarrhea, and, in rare instances, interstitial lung disease (Inoue *et al.*, 2013; Lacouture, 2006). All these clinical features were evident to some degree in our patient. Nevertheless, although skin papules and pustules developed during disease progression in our case, the early skin changes mostly consisted of erosions (which led to the erroneous initial clinical diagnosis of EB). EGFR signaling is known to be involved in the re-epithelialization phase of wound healing (Repertinger *et al.*, 2004; Pastore *et al.*, 2008), as well as the proliferation of keratinocyte stem cells (Jensen *et al.*, 2009), and we hypothesize that the missense mutation in our patient impeded these processes and was the primary cause of the erosive skin changes, with bacterial super-infection being a secondary contributing factor. The transcriptomic data from our patient illustrate the consequences of impaired EGFR signaling. The results (albeit based on RNA extracted from non-inflamed skin) reveal enhanced pro-inflammatory activation and disturbed differentiation/premature terminal differentiation of keratinocytes as key pathogenic mechanisms, thereby demonstrating a similar profile to that associated with the papulopustular rash associated with EGFR inhibitory drugs (Lacouture, 2006; Lichtenberger *et al.*, 2013; Mascia *et al.*, 2013). Notably, several inflammatory/innate response networks were significantly up-regulated, including NF-κB.

In conclusion, the EGFR network is one of the most influential and intricate signaling systems in biology. We believe the protean features in our patient offer clinical insight into the critical and diverse roles of EGFR, supporting many of the putative functions that have been ascribed to the receptor via murine models and *in vitro* studies. This case highlights the major mechanism of epithelial dysfunction following EGFR signaling ablation and illustrates the broader impact of EGFR inhibition on other tissues that might be under-appreciated in the context of concurrent malignancy in patients receiving EGFR inhibitor medications.

MATERIALS AND METHODS

Transmission electron microscopy

Small pieces of skin (<2mm^3) were prepared for transmission electron microscopy, as described in the Supplementary Material.

Immunofluorescence microscopy

A skin biopsy from the affected infant and control skin were collected in Michel's medium. The methods for immunofluorescence microscopy and primary antibodies used are listed in the Supplementary Material.

Whole-exome sequencing

Initially, 3 μg of genomic DNA was sheared with focused acoustic technology (Covaris, Woburn, MA, USA) to yield a mean fragment size of 150bp. Fragments ends were repaired

and sequencing adaptors ligated. Biotinylated 120bp RNA probes (Agilent, Santa Clara, CA, USA), designed against the coding regions of the genome were hybridized with the sequence library for 24 hours. DNA bound to RNA probes was retained using streptavidin-coated magnetic beads; unbound DNA was washed off. The exome-enriched pool of DNA was eluted and amplified with a low-cycle PCR. The DNA fragments were then sequenced with 100 bp paired-end reads. Novoalign (Novocraft technologies, Selangor, Malaysia) was used to align reads to the reference genome (hg19, National Center for Biotechnology Information build 37). With over 7.0 Gb of sequence generated, more than 90% of coding bases of the GENCODE-defined exome were represented by at least 20 reads (see Supplementary Material).

Sanger sequencing

We sequenced the exon and intron/exon boundaries of all 28 exons of *EGFR*, including the mutation present in exon 11, in the infant, mother, unaffected older brother and 3 controls. Each exon was amplified by PCR using AmpliTaq Gold® 360 Master Mix (Applied Biosystems, Foster City, CA, USA) and the primers listed in the Supplementary Material.

Whole-genome expression microarray analysis

Whole-genome expression microarray analysis was performed using RNA extracted from skin biopsies sampled from the affected child as well as 4 pooled, healthy controls. RNA extraction from cutaneous biopsies was performed using the Ambion mirVana miRNA Isolation kit (Invitrogen, Paisley, UK) according to the manufacturer's instructions. RNA was amplified using the Illumina TotalPrep RNA Amplification Kit (Illumina, San Diego, CA, USA) and subsequent gene expression profiling was performed using the Illumina array HumanHT-12 v4.0 Expression BeadChip kit according to the manufacturer's instructions (Illumina). Gene expression data were then analyzed using GenomeStudio software (Illumina). Control samples were pooled and compared to the affected individual.

Mutant construct transfection

Mutant complementary cDNA mimicking the mutation of the infant (c.1283G>A) was generated with green fluorescent protein (GFP) tagged to the C-terminus of EGFR. Wild type EGFR1-GFP was a gift from Dr Andrew Reynolds (Institute for Cancer Research, London, UK). The mutant construct, p.Gly428Asp EGFR-GFP was generated using a site-directed mutagenesis kit (Stratagene, La Jolla, CA, USA) as per the manufacturer's instructions using the following mutagenesis primer: 5′ GAGAACCTAGAAATCATACGCGACAGGACCAAGCAACATGGT-3′. The mutation in the plasmid was verified by sequencing. Transfection was carried out using Fugene (Roche Applied Science, Penzberg, Germany) or Lipofectamine (Invitrogen) reagents according to manufacturer's instructions.

Confocal microscopy

For confocal microscopy, cultured MCF-7 human breast adenocarcinoma cells were transfected with wild-type EGFR-GFP or p.Gly428Asp EGFR-GFP washed with PBS, fixed with 4% paraformaldehyde (PFA) in PBS for 10 mins and then permeabilized with 0.2%

TritonX-100 for 10 mins. For EGF stimulation experiments, cells were incubated in serum-free media (Opti-MEM®; Gibco Life Technologies, Carlsbad, CA, USA) for 16h prior to stimulation with 100 ng/ml EGF for the indicated times. For endocytosis inhibition experiments, cells were treated for 1 hour with 10 μM Dynasore (Millipore, Billerica, MA, USA) or equivalent volume of dimethyl sulfoxide (DMSO) as a control prior to fixation. Where appropriate, cells were incubated with a primary antibody directed against the extracellular domain of EGFR for 2h followed by the relevant secondary antibodies conjugated to Alexafluor-568 and Phalloidin conjugated to Alexafluor 568 or 633 for 1h at room temperature.

Western blotting

Thirty-thousand MCF-7 or CHO cells per condition were cultured in either Dulbecco's modification of Eagle's medium (DMEM) alone or DMEM containing 10% fetal calf serum (10% FCS) and transfected with wild-type EGFR-GFP or p.Gly428Asp EGFR-GFP; 36h later, the cells were starved for 16h with Opti-MEM® (Gibco Life Technologies) before treatment with 100 ng/ml EGF for the appropriate times. Cells were then lysed in sample buffer containing 2-mercaptoethanol at room temperature. Lysates were immediately subjected to SDS-PAGE and blotted using nitrocellulose membrane. Blots were blocked and probed using p-ERK, ERK, p-Akt, Akt, p-EGFR and EGFR antibodies (Cell Signaling Technology, Beverly, MA, USA), as well as HSC-70 antibodies (Santa Cruz Biotechnology, Dallas, Texas, USA), using 3% milk/PBS-0.2%tween or 5%BSA/TBS-0.1%tween.

Growth assessment rates

Ten-thousand CHO cells per condition were cultured in DMEM containing 10% FCS for 24h before transfection with GFP alone, wild-type EGFR-GFP or p.Gly428Asp EGFR-GFP. Twenty-four hours later, the media was replaced with normal growth media (10% FCS), growth media minus FCS or growth media minus FCS supplemented with 100 ng/ml EGF. Cells were then either Hoechst treated and fixed immediately with 4% PFA or were fixed 24h later. Phase and Hoechst images of 5 fields of view per condition were taken using an Olympus IX71 widefield microscope with a 4× 0.13 NA air objective (Olympus, Tokyo, Japan). Images were then analyzed for total number of cells as well as GFP expressing cells. The number of GFP expressing cells was then normalized using the total number of cells per field of view and presented either as the average number of GFP expressing cells per condition or the growth rate per condition.

Supplementary Material

Refer to Web version on PubMed Central for supplementary material.

ACKNOWLEDGEMENTS

The Centre for Dermatology and Genetic Medicine is supported by a Wellcome Trust Strategic Award (reference number 098439/Z/12/Z). The work was also supported by the UK National Institute for Health Research (NIHR) Biomedical Research Centre based at Guy's and St Thomas' NHS Foundation Trust and King's College London, as well as DebRA UK, and the British Association of Dermatologists. The views expressed are those of the authors and not necessarily those of the NHS, the NIHR or the UK Department of Health. This study was also supported, in part, by the Great Britain Sasakawa Foundation (Award No. 4314) and Strategic Young Researcher Overseas Visits

Program for Accelerating Brain Circulation (S2404) from the Japan Society for the Promotion of Science. We also thank Dr. Venu Pullabhatla for assistance with transcriptomic data analysis and access.

Abbreviations

EGFR epidermal growth factor receptor

REFERENCES

Avraham R, Yarden Y. Feedback regulation of EGFR signalling: Decision making by early and delayed loops. Nat Rev Mol Cell Biol. 2011; 12:104–17. [PubMed: 21252999]

Adzhubei IA, Schmidt S, Peshkin L, et al. A method and server for predicting damaging missense mutations. Nat Methods. 2010; 7:248–9. [PubMed: 20354512]

Blaydon DC, Biancheri P, Di WL, et al. Inflammatory skin and bowel disease linked to ADAM17 deletion. N Engl J Med. 2011; 365:1502–8. [PubMed: 22010916]

Blobel CP. ADAMs: Key components in EGFR signalling and development. Nat Rev Mol Cell Biol. 2005; 6:32–43. [PubMed: 15688065]

Chavanas S, Bodener C, Rochat A, et al. Mutations in SPINK5, encoding a serine protease inhibitor, cause Netherton syndrome. Nat Genet. 2000; 25:141–2. [PubMed: 10835624]

Dawson JP, Berger MB, Lin CC, et al. Epidermal growth factor receptor dimerization and activation require ligand-induced conformational changes in the dimer interface. Mol Cell Biol. 2005; 25:7734–42. [PubMed: 16107719]

Dreux AC, Lamb DJ, Modjtahedi H, et al. The epidermal growth factor receptors and their family of ligands: Their putative role in atherogenesis. Atherosclerosis. 2006; 186:38–53. [PubMed: 16076471]

Fine JD, Eady RA, Bauer EA, et al. The classification of inherited epidermolysis bullosa (EB): Report of the third international consensus meeting on diagnosis and classification of EB. J Am Acad Dermatol. 2008; 58:931–50. [PubMed: 18374450]

Gschwind A, Fischer OM, Ullrich A. The discovery of receptor tyrosine kinases: Targets for cancer therapy. Nat Rev Cancer. 2004; 4:361–70. [PubMed: 15122207]

Hansen LA, Alexander N, Hogan ME, et al. Genetically null mice reveal a central role for epidermal growth factor receptor in the differentiation of the hair follicle and normal hair development. Am J Pathol. 1997; 150:1959–75. [PubMed: 9176390]

Inoue A, Saijo Y, Maemondo M, et al. Severe acute interstitial pneumonia and gefitinib. Lancet. 2003; 361:137–9. [PubMed: 12531582]

Jensen KB, Collins CA, Nascimento E, et al. Lrig1 expression defines a distinct multipotent stem cell population in mammalian epidermis. Cell Stem Cell. 2009; 4:427–39. [PubMed: 19427292]

Jost M, Kari C, Rodeck U. The EGF receptor - an essential regulator of multiple epidermal functions. Eur J Dermatol. 2000; 10:505–10. [PubMed: 11056418]

Jutten B, Rouschop KM. EGFR signaling and autophagy dependence for growth, survival, and therapy resistance. Cell Cycle. 2014; 13:42–51. [PubMed: 24335351]

Kumar A, Petri ET, Halmos B, et al. Structure and clinical relevance of the epidermal growth factor receptor in human cancer. J Clin Oncol. 2008; 26:1742–51. [PubMed: 18375904]

Lacouture ME. Mechanisms of cutaneous toxicities to EGFR inhibitors. Nat Rev Cancer. 2006; 6:803–12. [PubMed: 16990857]

Lee CS, Kim IS, Park JB, et al. The phox homology domain of phospholipase D activates dynamin GTPase activity and accelerates EGFR endocytosis. Nat Cell Biol. 2006; 8:477–84. [PubMed: 16622417]

Lichtenberger BM, Gerber PA, Holcmann M, et al. Epidermal EGFR controls cutaneous host defense and prevents inflammation. Sci Transl Med. 2013; 5:199ra111.

Liu HB, Wu Y, Lv TF, et al. Skin rash could predict the response to EGFR tyrosine kinase inhibitor and the prognosis for patients with non-small cell lung cancer: a systematic review and meta-analysis. PLoS One. 2013; 8:e55128. [PubMed: 23383079]

Macia E, Ehrlich M, Massol R, et al. Dynasore, a cell-permeable inhibitor of dynamin. Dev Cell. 2006; 10:839–50. [PubMed: 16740485]

Mascia F, Lam G, Keith C, et al. Genetic ablation of epidermal EGFR reveals the dynamic origin of adverse effects of anti-EGFR therapy. Sci Transl Med. 2013; 5:199ra110.

Miettinen PJ, Berger JE, Meneses J, et al. Epithelial immaturity and multiorgan failure in mice lacking epidermal growth factor receptor. Nature. 1995; 376:337–41. [PubMed: 7630400]

Nanba D, Toki F, Barrandon Y. Recent advances in the epidermal growth factor/ligand system biology on skin homeostasis and keratinocyte stem cell regulation. J Dermatol Sci. 2013; 72:81–6. [PubMed: 23819985]

Ng PC, Henikoff S. SIFT: Predicting amino acid changes that affect protein function. Nucleic Acids Res. 2003; 31:3812–4. [PubMed: 12824425]

Ogiso H, Ishitani R, Nureki O, et al. Crystal structure of the complex of human epidermal growth factor and receptor extracellular domains. Cell. 2002; 110:775–87. [PubMed: 12297050]

Perrotte P, Matsumoto T, Inoue K, et al. Anti-epidermal growth factor receptor antibody C225 inhibits angiogenesis in human transitional cell carcinoma growing orthotopically in nude mice. Clin Cancer Res. 1999; 5:257–65. [PubMed: 10037173]

Pastore S, Mascia F, Mariani V, et al. The epidermal growth factor receptor system in skin repair and inflammation. J Invest Dermatol. 2008; 128:1365–74. [PubMed: 18049451]

Peschon JJ, Slack JL, Reddy P, et al. An essential role for ectodomain shedding in mammalian development. Science. 1998; 282:1281–4. [PubMed: 9812885]

Petrof G, Mellerio JE, McGrath JA. Desmosomal genodermatoses. Br J Dermatol. 2012; 166:36–45. [PubMed: 21929534]

Repertinger SK, Campagnaro E, Fuhrman J, et al. EGFR enhances early healing after cutaneous incisional wounding. J Invest Dermatol. 2004; 123:982–9. [PubMed: 15482488]

Rodeck U, Jost M, Kari C, et al. EGF-R dependent regulation of keratinocyte survival. J Cell Sci. 1997; 110:113–21. [PubMed: 9044042]

Schneider MR, Werner S, Paus R, et al. Beyond wavy hairs: The epidermal growth factor receptor and its ligands in skin biology and pathology. Am J Pathol. 2008; 173:14–24. [PubMed: 18556782]

Schneider MR, Wolf E. The epidermal growth factor receptor ligands at a glance. J Cell Physiol. 2009; 218:460–6. [PubMed: 19006176]

Sibilia M, Kroismayr R, Lichtenberger BM, et al. The epidermal growth factor receptor: From development to tumorigenesis. Differentiation. 2007; 75:770–87. [PubMed: 17999740]

Sibilia M, Wagner EF. Strain-dependent epithelial defects in mice lacking the EGF receptor. Science. 1995; 269:234–8. [PubMed: 7618085]

Stoll C, Alembik Y, Tchomakov D, et al. Severe hypernatraemic dehydration in an infant with Netherton syndrome. Genet Counsel. 2001; 12:237–43. [PubMed: 11693786]

Threadgill DW, Dlugosz AA, Hansen LA, et al. Targeted disruption of mouse EGF receptor: Effect of genetic background on mutant phenotype. Science. 1995; 269:230–4. [PubMed: 7618084]

Zhang Z, Xiao C, Gibson AM, et al. EGFR signaling blunts allergen-induced IL-6 production and Th17 responses in the skin and attenuates development and relapse of atopic dermatitis. J Immunol. 2014; 192:859–66. [PubMed: 24337738]

Europe PMC Funders Author Manuscripts

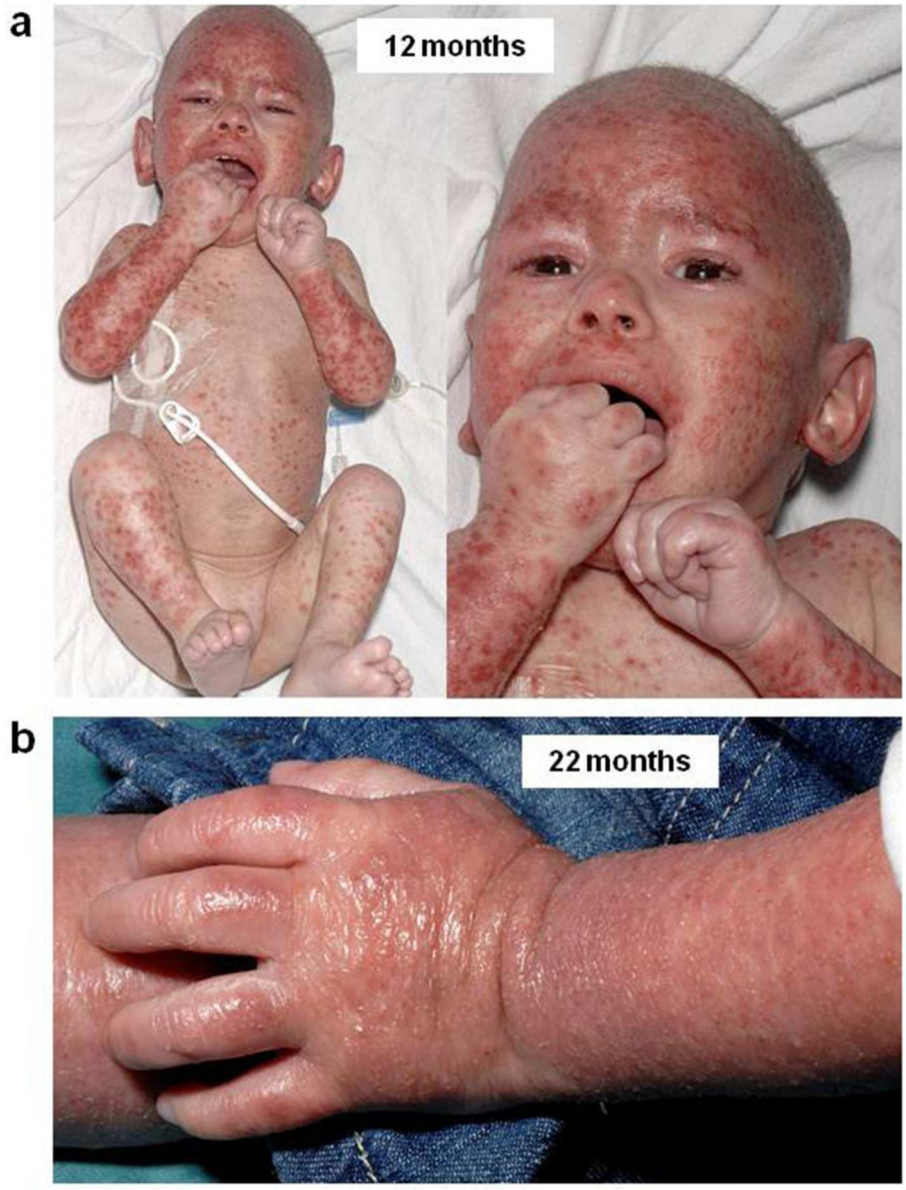

Figure 1. Clinical features of the patient demonstrating inflammation, erosions, papules and pustules

(**a**) At 12 months of age the infant has extensive erosions and markedly reduced scalp hair and eyebrows. He is also receiving total parenteral nutrition. (**b**) At 22 months there is a confluent papular eruption, particularly on the limbs, with numerous pustules. Consent to publish these photographs was obtained from the infant's mother.

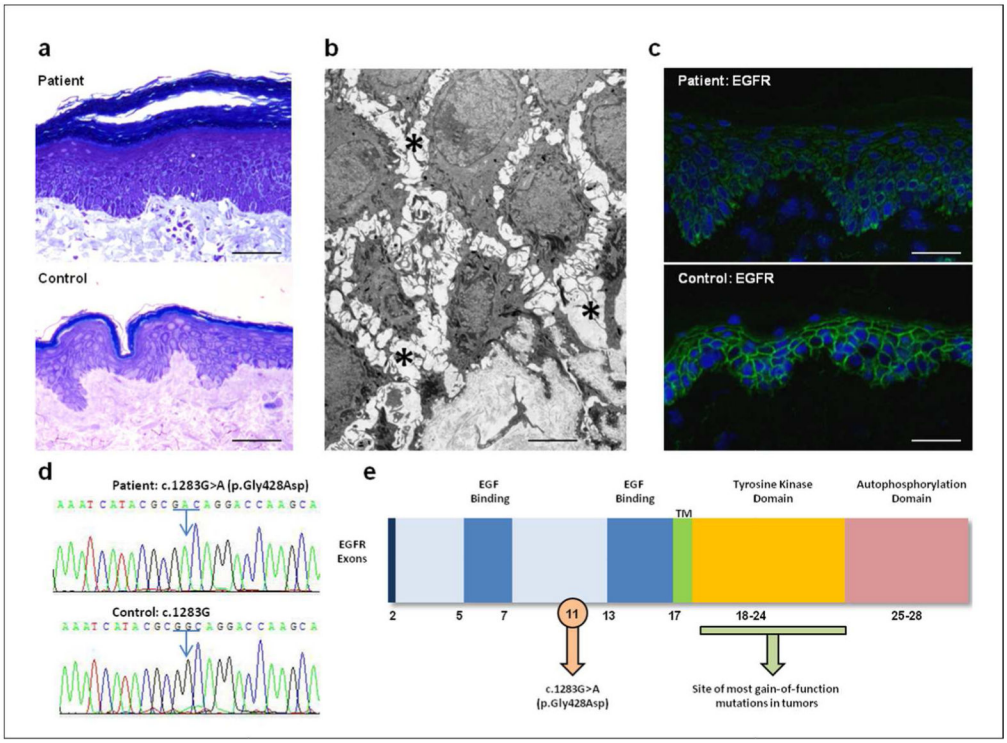

Figure 2. The homozygous mutation p.Gly428Asp results in acanthosis, intra-epidermal edema, and loss of keratinocyte cell membrane labeling for EGFR

(**a**) Semithin section of patient skin from the thigh reveals acanthosis and hyperkeratosis compared to age and site-matched control skin (scale bars = 50 μm). (**b**) Ultrastructurally, there is widening of spaces between adjacent keratinocytes in the lower epidermis (asterisks; scale bar = 2 μm). (**c**) Immunostaining for EGFR in patient epidermis shows loss of keratinocyte membrane staining compared to control skin (scale bars = 50 μm). (**d**) Sanger sequencing reveals a homozygous missense mutation in *EGFR*. (**e**) Schematic representation of the functional domains and encoding exons and the site of the pathogenic mutation in this patient. TM = transmembranous domain.

Europe PMC Funders Author Manuscripts

Europe PMC Funders Author Manuscripts

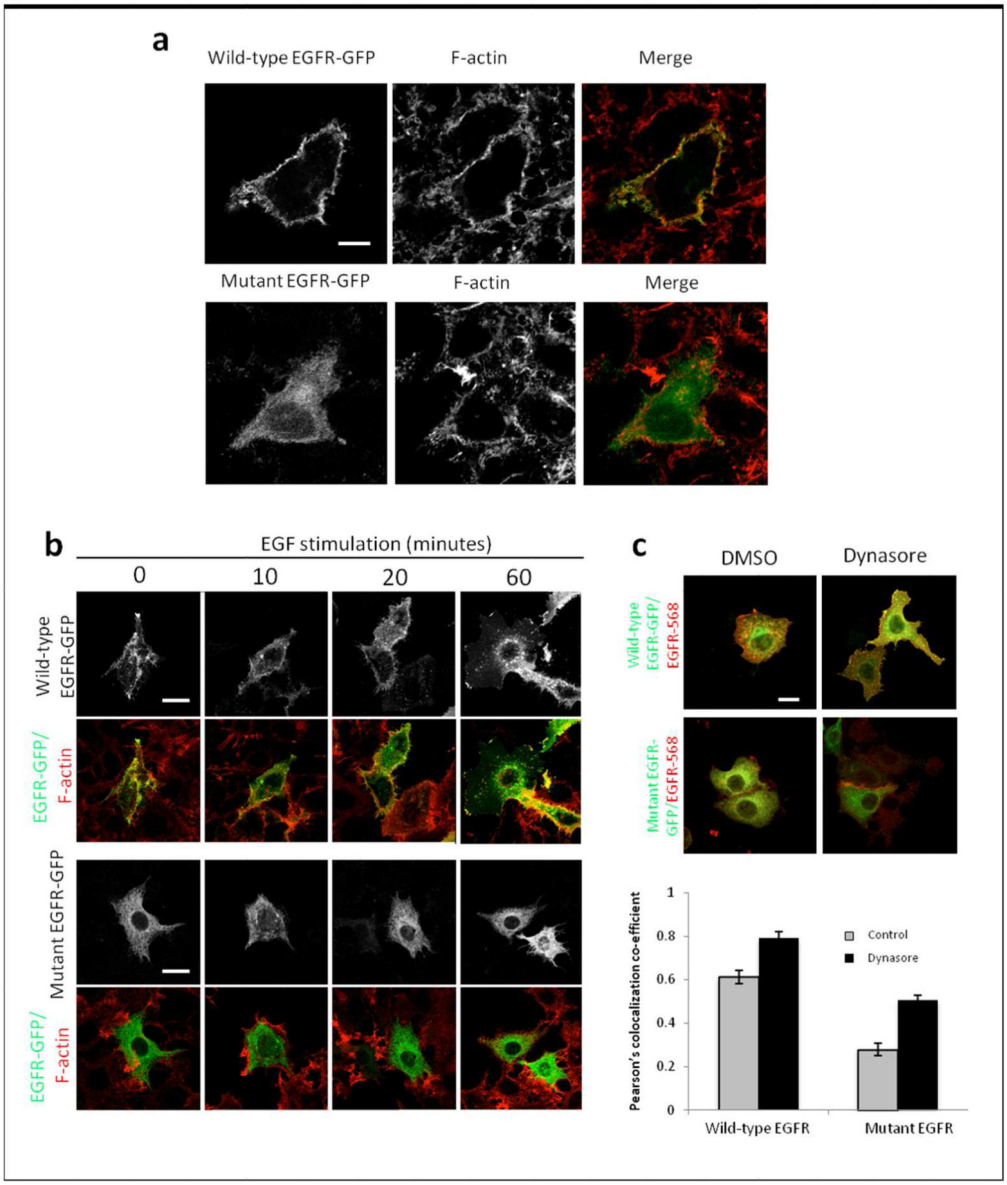

Figure 3. The mutation in *EGFR* renders the receptor unstable and susceptible to endocytosis

(**a**) Confocal microscopy was performed using GFP-tagged constructs of wild-type or mutant EGFR (green) and F-actin (red) in MCF-7 cells under normal growth conditions. (**b**) Images were then taken following stimulation of the cells with EGF at specified time points to assess the localization of EGFR within the cell cytoplasm or at the cell membrane. (**c**) Confocal microscope images were also taken for wild-type and mutant EGFR-GFP constructs (green) in cells stained for surface EGFR (red) in DMSO (dimethyl sulfoxide) control or Dynasore-treated cells (to inhibit endocytosis). The colocalization between EGFR antibody staining and either wild-type or mutant EGFR-GFP constructs was then quantified in DMSO control or Dynasore-treated cells using Pearson's correlation coefficient (Panel D lower). * $p<0.001$ vs WT-EGFR; scale bars = 10μm.

Europe PMC Funders Author Manuscripts

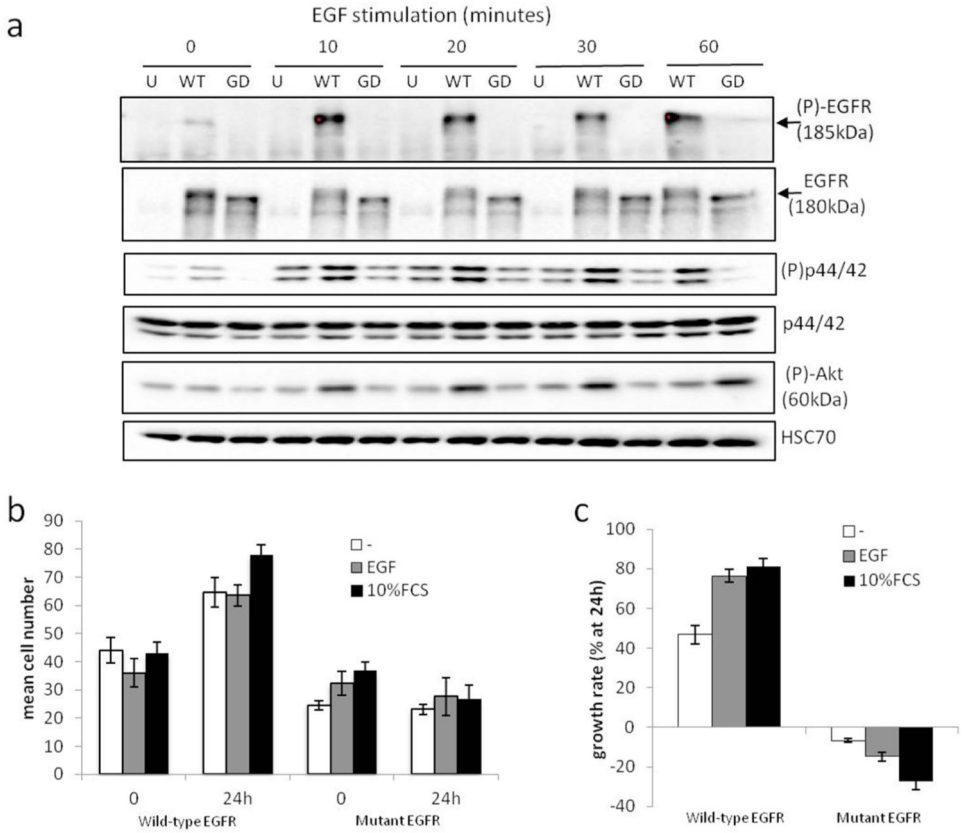

Figure 4. The mutation in *EGFR* reduces signal transduction and cell proliferation

(**a**) Western blotting was performed for p-EGFR, EGFR, p-ERK, ERK, p-Akt and Akt on lysates from untransfected (U), wild-type EGFR (WT) or mutant EGFR (MUT) transfected MCF-7 cells after EGF stimulation for the indicated times. MCF-7 cells express very low endogenous EGFR and therefore EGFR is undetectable in UT cells. Arrows indicate phospho and total EGFR species in top and second row blots respectively. Note the higher molecular weight species of EGFR in the WT samples in the second row blot are phosphorylated receptor and directly correlate with phosphorylated EGFR as detected in the top row blot. (**b**) Cell proliferation was quantified in CHO-K1 cells transfected with GFP, wild-type EGFR-GFP or mutant EGFR-GFP in starved (−), normal growth (10% fetal calf serum) or EGF-stimulated (EGF) conditions. (**c**) GFP-positive cells were counted and normalized against total cell number, and the cell growth rate was then calculated from these data.